

1  
2  
3  
4  
5  
6  
7  
8  
9  
10  
11  
12  
13  
14  
15  
16  
17  
18  
19  
20  
21

**Wind Driven Setup in East Central Florida’s Indian River Lagoon:  
Forcings and Pameterizations**

Jeffrey Colvin<sup>a</sup>, Steven Lazarus<sup>a</sup>, Michael Splitt<sup>b</sup>, Robert Weaver<sup>a</sup>, Peyman Taeb<sup>a</sup>

AFFILIATIONS

<sup>a</sup>Department of Ocean Engineering and Marine Sciences

<sup>b</sup>College of Aeronautics

Florida Institute of Technology  
150 W. University Blvd.  
Melbourne, FL 32901, USA

CORRESPONDING AUTHOR

Jeffrey A. Colvin

Department of Ocean Engineering and Marine Sciences  
Florida Institute of Technology  
150 W. University Blvd.  
Melbourne, FL 32901, USA  
Email: jcolvin2012@my.fit.edu

22 **ABSTRACT**

23 High resolution hydrodynamic models are computationally expensive to run – especially if  
24 ensemble forecasts are desired. This can be problematic within coastal estuaries which are not  
25 well resolved by today’s operational meteorological forecast models. As an alternative, this  
26 paper evaluates the wind forcing for three setup parameterizations (based on the Zuiderzee,  
27 modified Zuiderzee, and long wave equations) using a combination of observed setup from in-  
28 situ water level gauges and local wind observations. In addition, three methods are explored for  
29 developing hourly time series of wind forcing from 5-minute observations: top of the hour,  
30 hourly mean, and wind run approach. The wind forcings, which are weighted by the length of  
31 two lagoon-oriented axes, are used to drive the setup parameterizations. The observed setup is  
32 used to tune each of the parameterizations via a least squares approach. The observation spread,  
33 linear model residuals, coefficient of determination ( $R^2$ ), and root mean squared error (RMSE)  
34 indicate that the wind run out performs the other two methods. In terms of the three  
35 parameterizations, the modified Zuiderzee had consistently higher  $R^2$  values, lower RMSE, and  
36 narrower 95% confidence intervals than the two other methods. This optimized parameterization  
37 is currently being used operationally to generate ensemble setup forecasts for the Indian River  
38 Lagoon, a restricted estuary on Florida’s east-central coast. These simple ensemble forecasts are  
39 designed to guide the National Weather Service (NWS) in identifying potentially significant  
40 setup events that warrant high resolution hydrodynamic simulations.

## 41 **1. Introduction**

42 The National Weather Service (NWS) Nearshore Wave Prediction System (NWPS, van der  
43 Westhuysen et al. 2013), is designed to provide high resolution nearshore model guidance to  
44 coastal weather forecast offices. As a result, the NWPS does not include a hydrodynamic  
45 component and does not extend beyond the shoreline into coastal estuaries. Given the complex  
46 land-water mask and coastal geometry, hydrodynamic models require high spatial resolution  
47 (Weaver et al., 2016b), making them computationally expensive to run, particularly for ensemble  
48 forecasting. For example, the National Centers for Environmental Prediction (NCEP) has two  
49 operational atmospheric ensemble forecast systems including the Short Range Ensemble  
50 Forecast (SREF, Du and Tracton 2001) and the Global Ensemble Forecast System (GEFS, Toth  
51 and Kalnay 1993), both of which have more than 20 members. While it is not practical to run  
52 the full suite of hydrodynamic simulations on a high-resolution grid using wind forcing from  
53 each of the atmospheric ensemble members, a probabilistic approach that captures the magnitude  
54 and uncertainty associated with high impact wind events, remains attractive. An inexpensive  
55 setup parameterization can serve as a proxy to generate probabilities for setup and wave height  
56 inside the coastal zone. Use of parameterizations because of their computational efficiency is not  
57 uncommon (e.g., Apotsos et al. (2008) tested and calibrated several widely used wave  
58 parameterizations for coastal management). The objective here is to develop and tune a system  
59 that can be forced by ensemble wind forecasts. In addition, the probabilistic product can be used  
60 to determine whether resources for a high resolution hydrodynamic model run are warranted and  
61 in the subsequent selection of the relevant wind forcing (i.e., a particular ensemble member) for a  
62 deterministic water level forecast. The goal is not to replace hydrodynamic models but rather to  
63 facilitate their use.

64

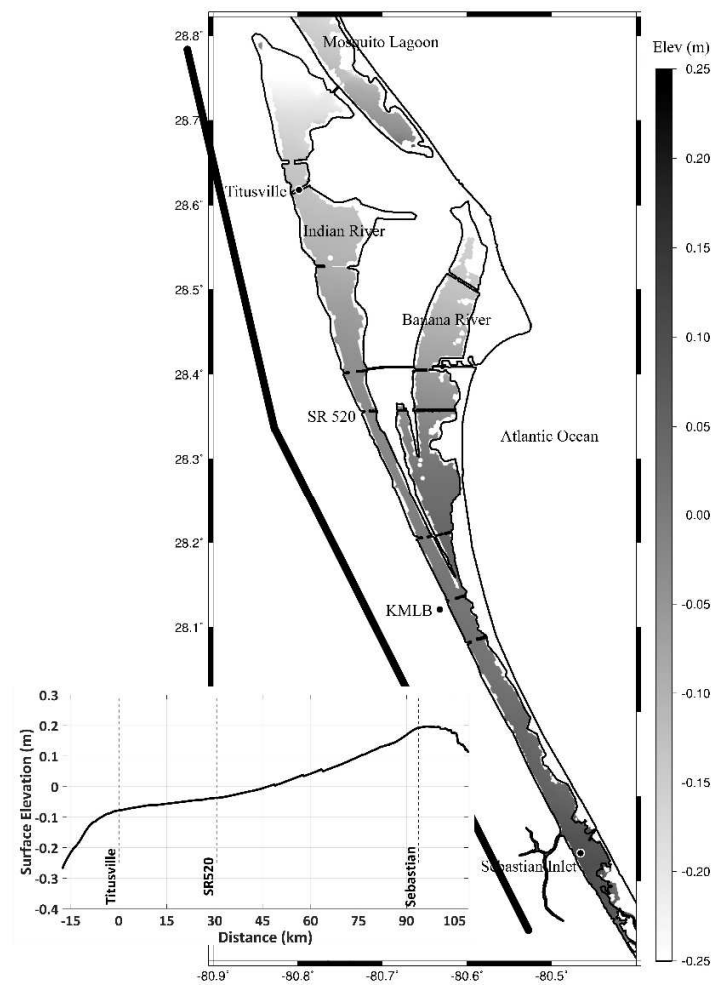
65 For the most part, setup parameterizations are used for engineering design (structural) purposes  
66 with a focus on threshold exceedance, i.e., what magnitude of wind speed, fetch and depth  
67 produce critical setup (Mostertman, 1963). The approach here is somewhat different since the  
68 focus is geared towards ensemble forecasting and model guidance. As a result, effort is spent in  
69 the development and evaluation of representative wind forcing that accounts for the local  
70 geometry, i.e., the lagoon orientation. Three different averaging methods are applied to surface  
71 wind observations and then used to force three setup parameterizations.

72

73 The Indian River Lagoon (IRL), located in east-central Florida (Fig. 1), is long (195 km),  
74 shallow (1-3 m), narrow (2-4 km), and has five inlets that connect it with the ocean, making it a  
75 restricted lagoon system (Kjerfve, 1986). In general, water movement in estuaries is influenced  
76 by atmospheric forcing, tidal action, and freshwater runoff (Reynolds-Fleming and Luettich,  
77 2004). However, because of the restricted nature and orientation of the lagoon, the effects of  
78 tidal forcing are reduced and thus the IRL is primarily wind driven (Smith, 1990). Given its  
79 narrow geometry, the IRL is extremely fetch limited with its orientation providing setup  
80 favorable conditions only in the presence of persistent southeast (or northwest) winds. These  
81 events can cause local flooding along the IRL, property damage, erosion, and impact water  
82 quality as a result of enhanced nutrient loading, resuspension, and sediment transport. In terms of  
83 the latter, Csanaday (1973) examined water motion forced by wind stress on long lakes (where  
84 the depth contours run parallel to the shores, similar to the IRL) and concluded that, in nearshore  
85 areas, the wind-forced component of the flow dominates. In fact, the wind-forced component  
86 was more important in transport than either seiching or oscillating movements, both of which are

87 present in the IRL (Weaver et al., 2016a). Additionally, downwind-driven water level increases  
88 are able to support substantially higher wave heights given the depth-limited nature of the IRL.  
89 Our data show it is not uncommon to see water level increases on the order of 40-50 cm during  
90 frontal passages or approaching cyclones, yielding a near 50% increase in water levels in some  
91 locations along the IRL.

92



93

94 Fig. 1. The northern Indian River Lagoon (IRL) basin of study including: the sensor locations,  
95 (Titusville and Sebastian Inlet), and the Melbourne National Weather Service Automated Surface  
96 Observing Station, KMLB. The bold black line approximates the orientation of the two lagoon

97 axes (see text for details). Also shown are the water elevation anomalies (m, shaded) and a  
98 surface elevation transect (m, inset) from ADCIRC+SWAN during the peak setup on 7 March  
99 2015.

100

101 A brief overview of the setup parameterizations is presented, followed by a description of the  
102 observational datasets (water level and winds). The wind averaging methodology, the  
103 identification of setup events, and a least squares approach that regresses the observed setup  
104 against the parameterized estimates for the different wind methods are then discussed. Finally,  
105 the wind forcing is evaluated using the best performing parameterization along with a brief  
106 summary and short discussion regarding potential forecast applications.

107

## 108 **2. Methodology**

### 109 **2.1 Setup Parameterizations**

#### 110 **2.1.1 The Zuiderzee Equation**

111 The equilibrium condition between the wind stress on the water surface and the pressure gradient  
112 generated by the slope of the free surface is expressed as the ratio of the kinetic energy of the  
113 wind stress,  $k\rho_a U^2$  (where  $k$  is the friction coefficient,  $\rho_a$  is the density of air, and  $U$  is the wind  
114 speed), and the potential energy of the water level increase,  $\rho g d$  (where  $\rho$  is the density of water,  
115  $g$  is the acceleration of gravity, and  $d$  is the water depth). This ratio, which represents the setup  $S$   
116 over the fetch  $F$ , is defined as

$$117 \quad \frac{S}{F} = 0.4 \times 10^{-6} \frac{U^2}{d}, \quad (1)$$

118

119 where  $k\rho_a/(\rho g) = 0.4 \times 10^{-6}$  (Mostertman, 1963). The friction coefficient  $k (= 0.003)$  was

120 obtained from measurements on the Zuiderzee as well as other lakes in Holland. Eq. (1) can be  
121 transformed into the well-known Zuiderzee relationship by letting  $a = k\rho_a/(\rho g)$  and expressing  
122 the setup as a function of wind speed, fetch, and water depth, i.e.,

123

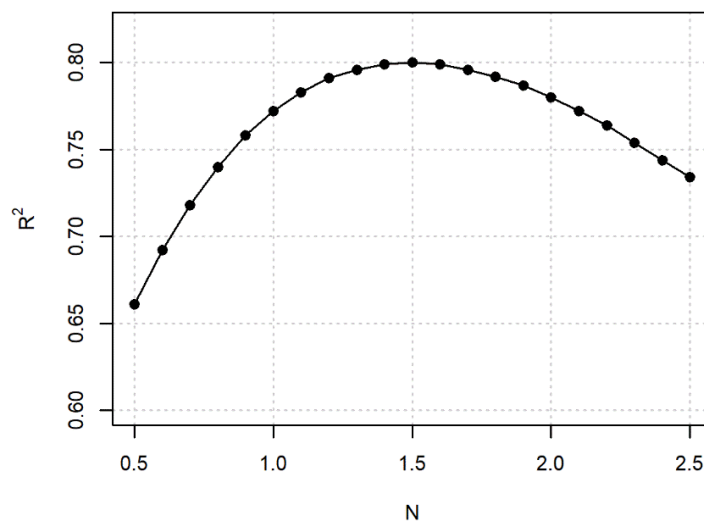
$$124 \quad S = a \frac{U^2 F}{d}. \quad (2)$$

125

### 126 **2.1.2 The Modified Zuiderzee**

127 While many studies relate the setup to the square of the wind speed, Harris (1963) suggested that  
128 strong correlations can also be found using powers of the wind ranging from one to two. To  
129 examine this here, the Zuiderzee is modified by setting  $U^2$  equal to  $U^N$  in Eq. (2). In order to  
130 determine the optimal power  $N$  in the modified Zuiderzee equation, wind forcing is inserted  
131 while systematically varying  $N$  from 0.5 to 2.5 in increments of 0.1. For each value of  $N$ , the  
132 predicted setup was regressed against the observed and the corresponding  $R^2$  values were then  
133 used to identify the optimum power (=1.5, Fig. 2).

134



135

136 Fig. 2.  $R^2$  values obtained from regressions of the observed versus parameterized setup for  
137 differing values of the wind speed exponent in the modified Zuiderzee parameterization (Eq. 2,  
138 with  $U^2$  equal to  $U^N$ ).

139

### 140 2.1.3 The Long Wave Equations

141 Water level changes induced by wind blowing over a water surface can also be described by the  
142 long wave equations (LWE) (Freeman et al., 1957). In this simple model, surface wind stress  
143 generates a current in the direction of the wind that, in turn, produces return flow in the opposite  
144 direction at the bottom of the water column. This counter current has a bottom stress associated  
145 with it that is usually unknown and not easily calculated (Sorensen, 2006). Both Saville (1952)  
146 and van Dorn (1953) found that the bottom stress was about 10% of the surface stress. Assuming  
147 steady state flow, the long wave equations simplify into a balance between the surface stress,  
148 bottom stress, and the pressure gradient of the sloping water surface (the addition of bottom  
149 stress distinguishes this approach from the Zuiderzee). The surface wind stress,  $\tau_s$ , is given by

150

$$151 \tau_s = k_s \rho U^2, \quad (3)$$

152

153 where  $k_s$  is the friction coefficient and  $\rho$  the water density. While Eq. (3) can also be written  
154 in terms of air density (Wu, 1969), this study uses Van Dorn's (1953) approach because it is  
155 more useful for looking at wind setup. For wind speeds greater than or equal to  $5.6 \text{ m s}^{-1}$ , Van  
156 Dorn's (1953) expression for the friction coefficient is given by

157

$$158 k_s = 1.21 \times 10^{-6} + 2.25 \times 10^{-6} \left(1 - \frac{5.6}{U}\right)^2. \quad (4)$$



159

160 At wind speeds below  $5.6 \text{ m s}^{-1}$ ,  $k_s$  is assumed to be constant ( $= 1.21 \times 10^{-6}$ ), while for wind  
161 speeds greater than or equal to  $5.6 \text{ m s}^{-1}$ ,  $k_s$  asymptotically increases (to  $3.46 \times 10^{-6}$ ) to account  
162 for increased roughness as waves form on the surface.

163

164 The LWE setup as developed in Dean and Dalrymple (1990) and Sorensen (2006) is given by

165

$$166 \quad S = d \left( \sqrt{\frac{2k_{sb}U^2F}{gd^2} + 1} - 1 \right), \quad (5)$$

167

168 where  $k_{sb}$  is a combined surface/bottom stress coefficient. This study uses Eq. (4) to calculate  
169 the surface stress from the wind speed. This value is then multiplied by 1.1 to obtain an estimate  
170 of  $k_{sb}$  (Sorensen, 2006). The setup prediction from Eq. (5) is hereinafter referred to as the *long*  
171 *wave* method.

172

## 173 **2.2 Water level**

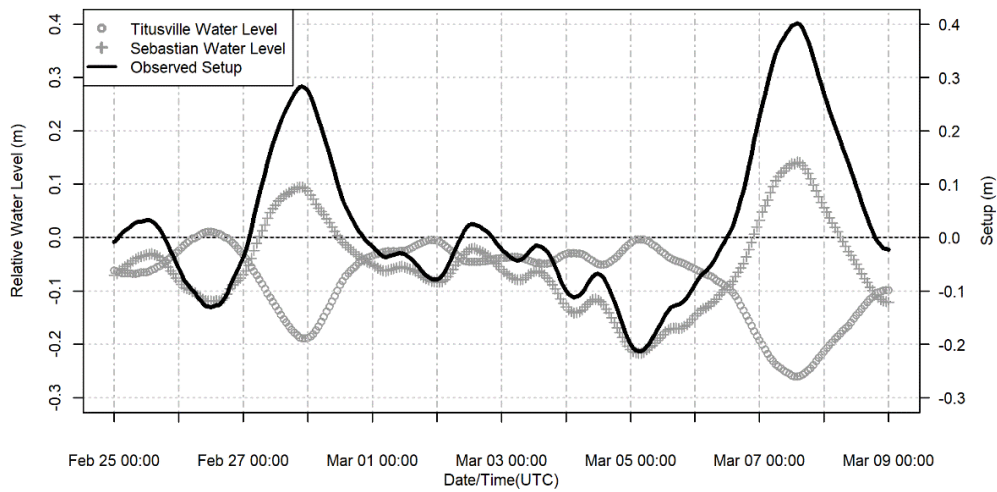
174 Two water level gauges, located near Sebastian Inlet to the south and Titusville to the north  
175 (about 100 km apart), were used to calculate water level differences and thus estimate the  
176 observed wind setup between the two locations (Fig. 1). A HOBO U20 titanium water level  
177 pressure sensor was deployed in a PVC tube stilling well near the Sebastian Inlet, while the  
178 northern sensor near Titusville is maintained by the St. Johns River Water Management District.  
179 Sensors at both locations provide hourly water level data. To correct for atmospheric effects on  
180 the water level, the hourly barometric pressure observations from the Melbourne (KMLB)  
181 National Weather Service Automated Surface Observing Station (ASOS, Fig. 1) were subtracted

182 from the sensor pressure measurements. This approach is generally robust along the IRL as  
183 pressure variations are on the order of 1 mb or less between KMLB and the Titusville ASOS  
184 (KTIX, not shown). Assuming a hydrostatic pressure response, the adjusted pressure is converted  
185 to a relative water level (i.e., height above instrument). The data used for this investigation were  
186 collected from November 2014 to March 2015 and from November 2015 to March 2016. Frontal  
187 passages leading to significant setup events are common during these months. Additionally, the  
188 time period selected spans Florida's dry season, and thus, should lessen the impact of storm  
189 water runoff on water levels.

190

191 The relative water level is expressed in terms of anomalies, which are calculated by subtracting  
192 the hourly measurements from the seasonal (November to March) mean. Although some  
193 formulations reference setup from still water level, here it is defined to be consistent with its  
194 original interpretation (Mostertman, 1963) i.e., as the difference between the relative water levels  
195 on the downwind and upwind portions of the basin. A simple twelve-hour running mean was  
196 applied to filter the tidal signal at the sensor near Sebastian Inlet. This method produced results  
197 comparable to that of harmonic analysis software -- removing high frequency wind waves, boat  
198 wakes, etc. Because the water level at Titusville is subtracted from that of Sebastian, the  
199 observed setup is defined as positive for northerly flow (set down in Titusville, setup in  
200 Sebastian) and negative for southerly flow (set down in Sebastian, setup in Titusville) as shown  
201 in Figure 3.

202



203

204 Fig. 3. Water level data for the Titusville station (open circles) and the Sebastian Inlet station

205 (crosses) for 25 February - 9 March 2015. The observed setup is calculated by subtracting

206 Titusville from Sebastian, yielding positive/negative setup for a northerly/southerly wind event

207 (black line).

208

### 209 2.3 Wind

210 The wind from the KMLB ASOS is used to force the three setup parameterizations examined

211 herein. Although the station is centrally located, it is inland, and thus may not be representative

212 of the over water winds that drive setup in the IRL. This issue is addressed in more detail in the

213 context of tuning the parameterizations presented in Section 2.4. Comparisons using in-situ open

214 fetch winds from WeatherFlow station data within the IRL produced similar results (not shown),

215 hence only KMLB winds are presented here.

216

217 The IRL is long and narrow and thus extremely fetch limited in most locations with fetch

218 lengths, even for the most favorable flow directions, generally less than 10 km (Holman et al.,

219 2017). While each of the setup parameterizations depend on the wind speed, it is the along-  
220 lagoon component of the wind that is ultimately responsible for setup. Furthermore, the constant  
221 direction assumption regarding fetch is complicated somewhat by the geometry of the portion of  
222 the IRL under consideration here. To account for a change in the orientation of the major axis of  
223 the lagoon, an along-estuary wind component is calculated by projecting the observed wind onto  
224 two distinct fetch-weighted segments (Fig. 1). The respective wind components for each section  
225 are then calculated separately by multiplying the KMLB wind speed by the cosine of the angle  
226 between the wind direction and the relevant lagoon axis. A single lagoon representative wind  $U_R$   
227 is constructed by weighting each of the components ( $U_1$  and  $U_2$ ) by their respective fetch lengths  
228 ( $F_1$  and  $F_2$ ), i.e.,

$$229 \quad U_R = \left( \frac{U_1 F_1 + U_2 F_2}{F_1 + F_2} \right). \quad (6)$$

230  
231 The approach of breaking the estuary into two segments yielded slightly higher correlation  
232 values (between observed and predicted setup) than using just a single average angle and fetch  
233 length (not shown).

234  
235 In order to match the temporal scale of the water level observations, three different averaging  
236 methods were used to generate hourly time series from the five-minute KMLB wind data. In  
237 addition, the hourly wind forcing is more consistent with respect to ensemble wind forecasts,  
238 which generally have a three or six-hour temporal resolution. The three wind averaging methods  
239 include: top of the hour, hourly mean, and wind run. The top of the hour method uses the wind  
240 speed and direction nearest to the beginning of the hour. The hourly mean method calculates a  
241 vector mean speed and direction for the prior hour. The wind run is comprised of a running

242 average over a specified time period. In this study, an antecedent twelve-hour window is used  
243 (other intervals were explored but the 12 h performed best). The u and v components are  
244 averaged separately and then recombined to produce the wind run forcing. The wind run is the  
245 only method of the three explored that considers a wind duration longer than an hour.

246

#### 247 **2.4 Tuning the Setup Parameterizations**

248 In order to identify setup events, a centered rolling extrema function with a temporal width of 9 h  
249 was applied to determine if the observed setup was a local maximum or minimum within the  
250 prescribed time window (i.e.,  $\pm 4$  h of the current observation time). The resulting extrema  
251 were initially selected using a subjective setup threshold of  $\pm 10$  cm. However, this leaves a  
252 data gap with respect to low amplitude events (i.e., less than 10 cm) and inflates the  $R^2$  values.  
253 As a result, a threshold of 1 cm is used instead. The addition of the low-end events produces  
254 robust regression statistics, with only slight changes the values of the slopes or intercepts.  
255 Overall, 350 events were identified, but eight were removed because either some or all of the  
256 wind speed data were missing prior to the setup time. Three distinct wind forcing time series,  
257 associated with the 342 events, were calculated by inserting the wind speeds from the – top of  
258 the hour, hourly mean, and wind run – into Eq. (6). Since setup response to the wind forcing is  
259 not instantaneous (see lag discussion in Section 4), the maximum wind speed is selected from a  
260 period prior to the observed peak setup for both the top of the hour and hourly mean methods.  
261 Time intervals ranging from 6 to 18 hours were evaluated, with a 12-hour period producing the  
262 best results (i.e., lowest RMSE between the predicted and observed setup). A similar approach is  
263 applied to obtain the optimal averaging time period for the wind run method -- also 12-hours.

264

265 Each of the setup parameterizations depends on the water depth, which is typically taken to be  
 266 the average depth along the fetch. However, because this can be problematic for irregularly-  
 267 shaped basins, Sorensen (2006) suggests using the average depth of the basin. This study uses  
 268 the average depth ( $d = 1.2 \text{ m}$ ) for the northern section of the IRL (Titusville to Sebastian). If  
 269 depth and fetch (both constants) are incorporated into  $\alpha$ , the setup parameterizations can be  
 270 expressed as

271

272 Zuiderzee: 
$$S = \alpha U_R^2 + \beta, \quad (7)$$

273

274 Modified Zuiderzee: 
$$S = \alpha U_R^{1.5} + \beta, \text{ and} \quad (8)$$

275

276 Long Wave: 
$$S = \alpha \left( \sqrt{\frac{2k_{sb}U_R^2F}{gd^2} + 1} - 1 \right) + \beta. \quad (9)$$

277

278 where  $\alpha$  is the slope and  $\beta$  the intercept. The three wind forcings are then inserted into each of  
 279 the setup parameterizations with the output regressed against the corresponding observed setup.  
 280 The regression is straightforward and is accomplished by plotting the observed setup versus the  
 281 forcing in equations (7-9). This results in 9 distinct regression equations - one for each  
 282 combination of the individual wind forcings and parameterizations. The regression essentially  
 283 tunes the setup parameterizations to the IRL with the values of  $\alpha$  and  $\beta$  varying for each of the  
 284 parameterization and wind forcing pairings.

285

286 Because the heights of the water level gauges are not referenced to a vertical datum, the setup is  
 287 estimated using a local water level anomaly based on the seasonal mean at each gauge location.

288 Ideally, for each regression, the intercept,  $\beta$ , should be close to zero, i.e., no wind/no setup.  
 289 However, the seasonal prevailing winds will likely contribute to some nominal wind setup  
 290 between the two locations. A non-zero (positive) setup in the absence of wind forcing indicates  
 291 that the seasonal mean water level at the Sebastian Inlet sensor is higher than that at Titusville.  
 292 This systematic bias is evident, as a nonzero intercept (on the order of -3 cm), in the various  
 293 regressions (Table 1). An unbiased estimate of the regression setup coefficients requires that the  
 294 average difference between the observed and predicted setup over some time interval be close to  
 295 zero. Therefore, a 3 cm bias correction, which is within one standard deviation of the mean  
 296 observed setup with no wind forcing, is applied here. The bias corrected scatterplot and least-  
 297 squares fit for the wind run forced modified Zuiderzee parameterization is shown in Figure 4.  
 298 The regression parameters for each of the possible wind forcing/parameterization combinations  
 299 are presented in Table 1.

300

301

302

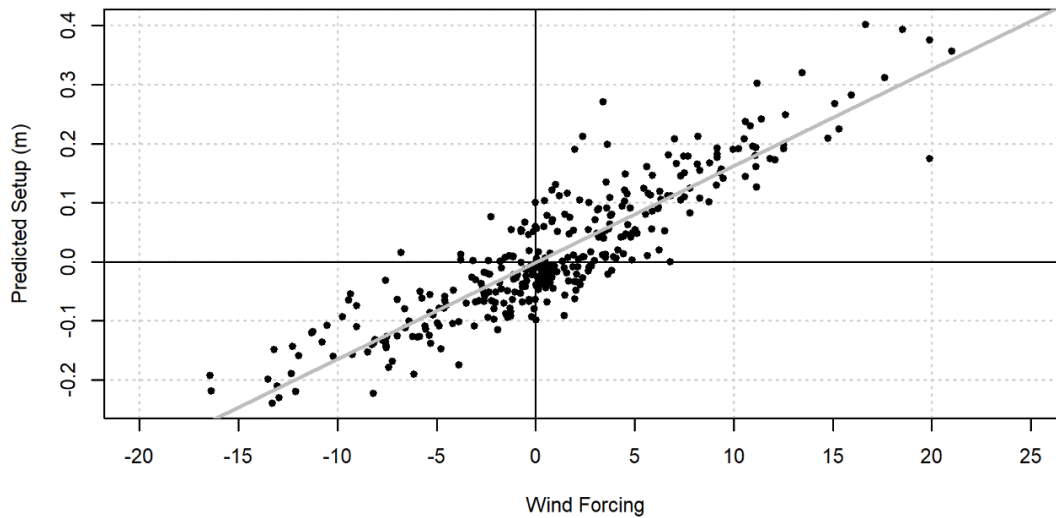
303

304 **Table 1**

305 Summary of regressions (no bias correction) and RMSE for each wind forcing/parameterization  
 306 pair. Highest  $R^2$  and lowest RMSE are in bold.

307	308	309	310	311	312	313
Forcing	Parameterization	$\alpha$ (slope)	$\beta$ (intercept)	$R^2$	RMSE (cm)	
Top of Hour	Zuiderzee	0.0048	-0.0277	0.5256	4.94	
	Mod. Zuiderzee	0.0122	-0.0286	<b>0.5790</b>	<b>4.46</b>	
	Long Wave	0.2943	-0.0300	0.5415	6.39	
Hourly Mean	Zuiderzee	0.0054	-0.0281	0.5762	4.74	

315		Mod. Zuiderzee	0.0130	-0.0287	<b>0.6170</b>	<b>4.34</b>
316		Long Wave	0.3187	-0.0296	0.5810	6.27
317						
318	Wind Run	Zuiderzee	0.0073	-0.0304	0.7800	3.85
319		Mod. Zuiderzee	0.0164	-0.0311	<b>0.8001</b>	<b>3.59</b>
320		Long Wave	0.7461	-0.0321	0.7582	5.98
321						
322						
323						



324

325 Fig. 4. Predicted set up (bias corrected) for the modified Zuiderzee with wind run forcing. The  
 326 black dots represent the 342 events in the training dataset, and the gray line is the least squares  
 327 fit.

328

### 329 3. Results

330 The tuning dataset is used to optimize the setup parameterizations using the different wind  
 331 forcing methods. Performance is evaluated using the  $R^2$  and RMSE statistical parameters.

332

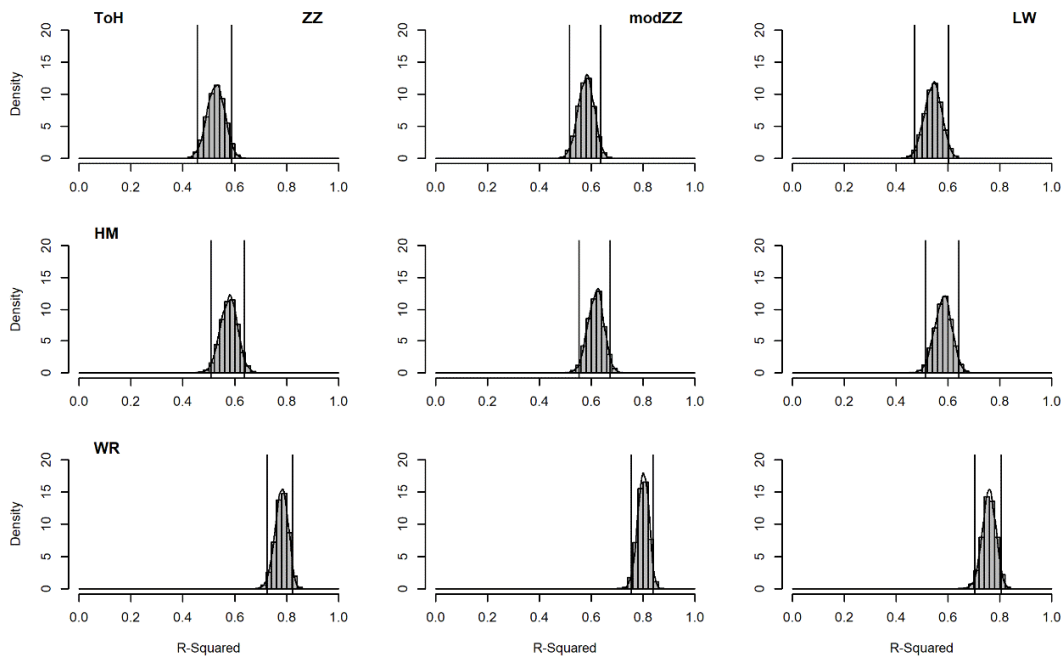
#### 333 3.1 Parameterization Performance

334 To evaluate the robustness of each regression, 5000  $R^2$  values were generated by bootstrapping



335 the tuning data (i.e., the 342 events). The density histograms from the bootstrapping are shown in  
 336 Figure 5. The 95% confidence interval (vertical lines) is tighter and the  $R^2$  larger for the three  
 337 wind run forced parameterizations. In addition to the significant increase in  $R^2$  for all three  
 338 parameterizations when forced with the wind run, a tighter confidence interval is also evident.  
 339 The modified Zuiderzee performs slightly better than the Zuiderzee and the long wave methods.  
 340 A bootstrapping approach was also applied by randomly subsampling our dataset to successively  
 341 reduce the number of events and examining the change in the width of the 95% confidence  
 342 intervals for the regression coefficients (i.e., slope and y-intercept) and  $R^2$  for 5000 samples. The  
 343 results (not shown) indicate that the widths of the confidence intervals decrease rapidly and then  
 344 flatten out at around 250 events, suggesting that our dataset (342 events) is robust in defining the  
 345 regression coefficients of our parameterizations.

346



347

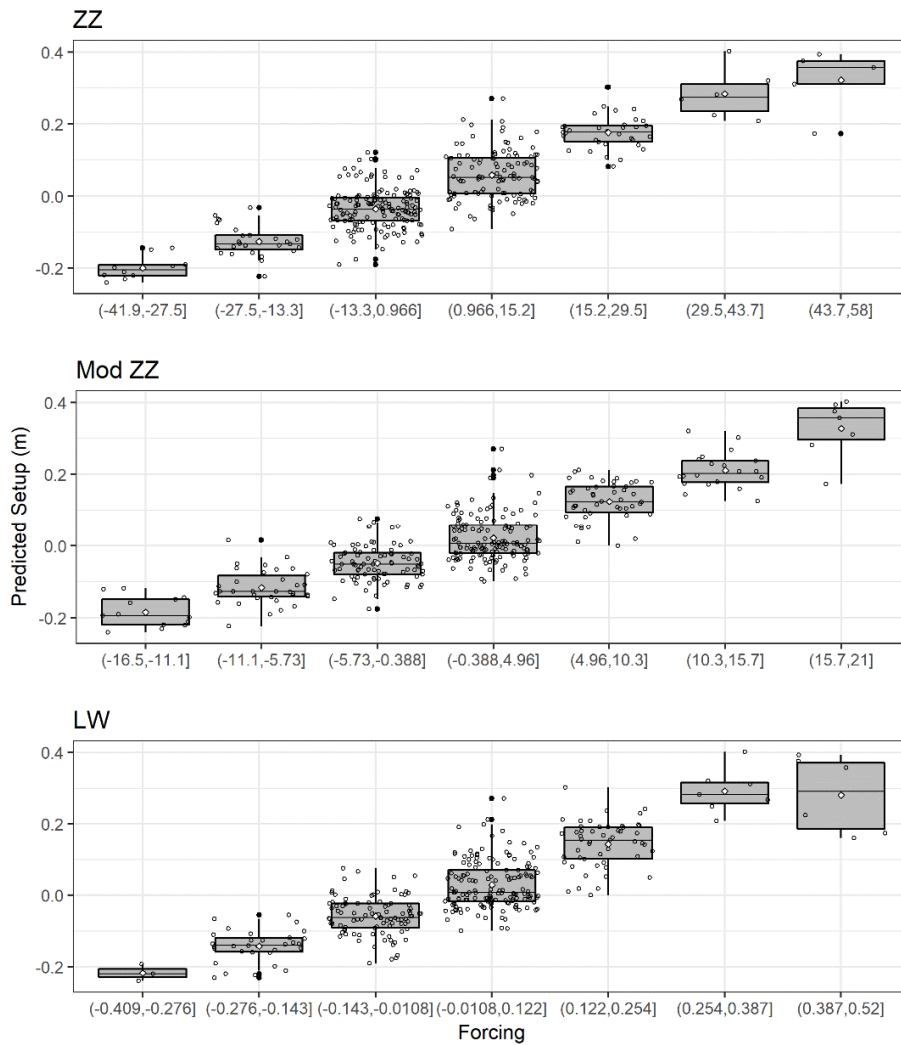
348 Fig. 5. Bootstrapped density histograms for the nine wind forcing/parameterization

349 combinations. Rows (from top-to-bottom) are the different wind forcing methods: top of the hour  
350 (ToH), hourly mean (HM), and wind run (WR). The columns (left-to-right) are the three setup  
351 parameterizations: Zuiderzee (ZZ), modified Zuiderzee (modZZ), and the long wave (LW). The  
352 vertical lines in each panel represent the 95% confidence intervals.

353

354 In addition to the regression statistics, a standard box plot of the predicted setup versus each of  
355 the wind run forced parameterizations is presented (Fig. 6). Here, each of the boxes has the same  
356 width and are populated with their respective predictions (open circles). The x-axes represent the  
357 independent variables for each parameterization (Eqs. 7-9). The outliers are depicted by the filled  
358 circles. The box plots indicate a degree of heteroscedasticity (e.g., a maximum variation in setup  
359 for low wind forcing in the Zuiderzee). The standard deviations of the box heights for each of the  
360 parameterizations, which represent the spread of the middle 50% of the forecast setup, vary from  
361 1-to-5 cm, with the modified Zuiderzee exhibiting the lowest variability. In addition, of the three  
362 parameterizations, the modified Zuiderzee exhibits greater consistency along the x-axis (i.e., a  
363 more even distribution).

364



365

366 Fig. 6. Boxplots for the three wind run forced setup parametrizations (top-to-bottom): Zuiderzee

367 (ZZ), modified Zuiderzee (modZZ), and long wave (LW). The shading represents the middle

368 50% of the data distribution (within equally-spaced intervals, x axis) and the whiskers depict the

369 upper and lower quartiles. The intervals (x-axis) represent the independent variables in equations

370 (7- 9). The median (mean) is given by the thin horizontal line (white diamond) within each box.

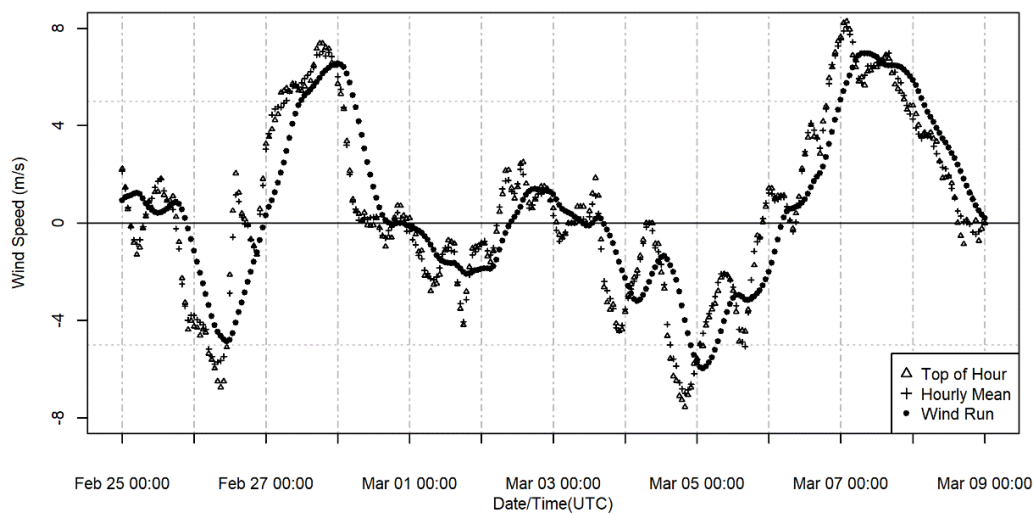
371 Open circles depict the spread of the data within the given intervals and outliers are indicated by

372 the solid black dots.

373

374 **3.2 Evaluation**

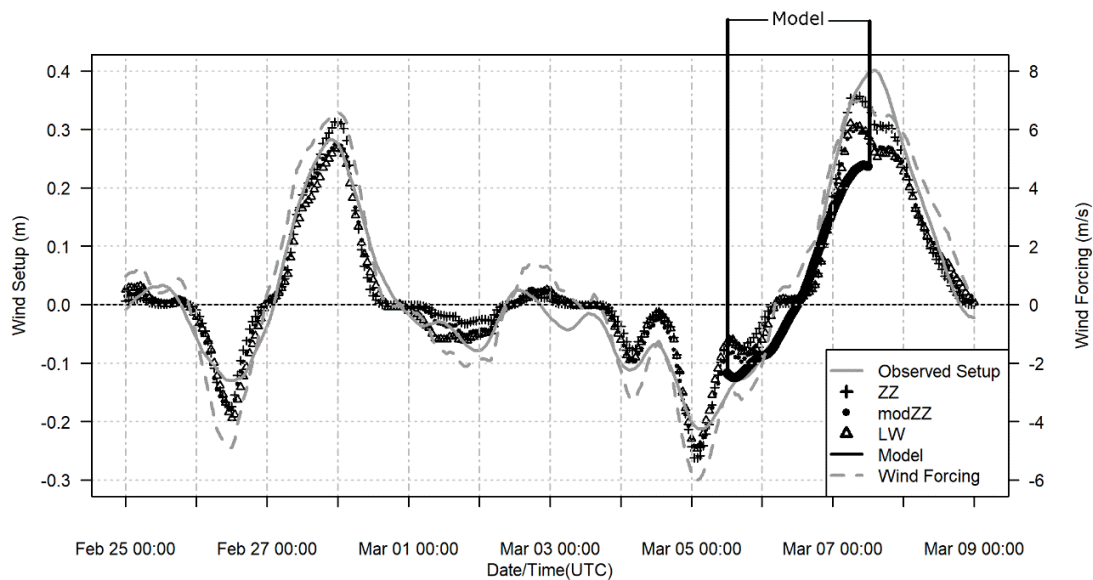
375 While for the tuning, the lag was accounted for by pairing the peak wind forcing with maximum  
376 setup for each of the events (see section 2.4), this will not be the case for the predicted setup. In  
377 terms of the latter, it would be advantageous to determine the wind forcing/water level response  
378 time scale for the IRL study region. Here, a standard cross-correlation technique is applied to  
379 estimate the lag. Our results indicate a peak correlation (on the order of 0.95) for a lag of 6 hours.  
380 This result is consistent for all three parameterizations and wind forcings – except for the wind  
381 run which does not require a lag adjustment (see Section 4). Ultimately, any inherent lag would  
382 need to be taken into account within a forecast environment.



383  
384 Fig. 7. Wind speeds (m/s) on 25 February - 9 March 2015 for the top of the hour (open triangles),  
385 the hourly mean (crosses) and the wind run (filled circles).

386  
387 In order to gauge the impact of the wind forcing on the predicted setup, the best performing  
388 parameterization, the modified Zuiderzee, is applied to a time period from 25 February – 10  
389 March 2015. This period is relatively active as it has four somewhat distinct setup events (i.e.,

390 setup > 10 cm). The wind speed time series computed using the three wind forcing methods is  
 391 shown in Figure 7. The top of the hour and hourly mean winds behave similarly, with the latter  
 392 showing a small reduction in the predicted peak wind speed. As expected the wind run method  
 393 acts as a temporal filter on the wind speed, but it also takes the wind duration into account. In  
 394 tandem, these two characteristics act to reduce the RMSE which is the lowest of the three  
 395 forcings (Table 1). The observed and predicted setup for each of the wind run forced  
 396 parameterizations is shown in Figure 8.



397  
 398 Fig. 8. Setup from the three wind run forced parameterizations including the Zuiderzee (crosses),  
 399 modified Zuiderzee (filled circles), and the long wave (open triangles). Also shown are the  
 400 observed setup (solid gray line) the wind run forcing (dashed gray line, right axis) for 25  
 401 February - 9 March 2015, and the predicted setup from the ADCIRC + SWAN for 12 UTC 5  
 402 March - 12 UTC 7 March (thick black line).

403  
 404

405 In order to relate the predicted setup to water levels throughout the lagoon, results from a  
406 coupled ADCIRC + SWAN (Booij et al., 1999; Luetlich, R.A., Jr., J.J. Westerink, 1992)  
407 hydrodynamic/wave model simulation are briefly presented here. The event period 5-7 March  
408 2015, captures a strong frontal passage. ADCIRC + SWAN was forced using a four member  
409 ensemble of winds with various spatial and temporal resolutions, generated from the Weather  
410 Research and Forecasting (WRF) model (see Weaver et al. 2016b for more details). As a direct  
411 comparison with the three parameterizations, ADCIRC water levels are mined at the Titusville  
412 and Sebastian gauge locations and their difference (setup) is shown in Figure 8, (bold black line  
413 labeled model). The phase (timing) of the model predicted setup is coeval with that of the  
414 parameterizations. The amplitudes of the modeled and the parameterized setup vary between 25  
415 and 35 cm, all of which under forecast the observed peak near 40 cm.

416

417 IRL water level anomalies during the peak setup (12 UTC 7 March) associated with post-frontal  
418 northerly flow is shown in Figure 1 (shaded). Water levels change somewhat gradually with  
419 maximum set down north of Titusville and peak setup in the flow constricted area southeast of  
420 Sebastian. In particular, the fetch favorable (northeast to southwest) orientation of the Banana  
421 River exhibits water level variations between 10-15 cm, while in northwest-to-southeast oriented  
422 Mosquito Lagoon the differences are on the order of 5 cm or less. Maximum setup in these  
423 portions of the estuary likely occurs at different times during the course of the wind event. The  
424 response in other regions of the IRL during the peak setup (as defined by our two locations) is  
425 somewhat less and depends on the respective fetch.

426

427 An ADCIRC+SWAN transect of water levels on the Indian River is shown in Figure 1 (inset).

428 This transect extends beyond the boundaries of the Titusville and Sebastian Inlet gauges used to

429 calculate the observed setup for the parameterizations. The two fetch segments (Section 2.3) are  
430 divided by route 520 which crosses the Indian River about 30 km south of the Titusville gauge  
431 location. As evident by the slope, the change in water levels from Titusville to SR520, a  
432 somewhat wider section of the Indian River, occurs more slowly than the change between SR520  
433 and Sebastian Inlet. A relatively large decrease in the water level occurs north of Titusville. This  
434 shallow portion of the lagoon is often blown down during periods of extended northerly flow.

435

#### 436 **4. Discussion and Conclusion**

437 The performance of the modified Zuiderzee parameterization was somewhat unexpected given  
438 that it does not directly account for bottom stress. However the LWE, which takes into account  
439 the effects of friction at the lower boundary (it is approximated assuming that it is 10% of the  
440 surface stress, i.e.  $k_{sb} = 1.1k_s$ , Eq. (4)), has slightly degraded results. A stress approximation  
441 similar to that of the LWE can be applied to the Zuiderzee methods. This would result in a trivial  
442 modification of the coefficient  $a$  in Eq. (2) by a constant multiplicative factor. While this would  
443 have an impact on the regression parameters, it would not affect the statistics (i.e.,  $R^2$ ). In this  
444 sense, the bottom stress is implicit in the Zuiderzee formulations.

445

446 The Zuiderzee was originally formulated to assess the impact of wind driven setup on structures  
447 using an exceedance value or some maximum expected wind speed (Ahrens, 1976; Mostertman,  
448 1963). In contrast, the approach here is predictive rather than diagnostic, i.e., input a forecast  
449 wind speed time series and output setup. As previously discussed, the relationship between the  
450 wind and setup may not be quadratic (Section 2.1.2). Here, this was examined using variable  
451 forcing in the form of setting  $U^2$  to  $U^N$  in Eq. (2). The best results (i.e., the highest  $R^2$ ) were

452 achieved for  $N=1.5$ . This non-standard formulation relating wind setup to  $U^{1.5}$  was referred to as  
453 the modified Zuiderzee herein. Why the modified Zuiderzee performs slightly better is not clear.  
454 As previously mentioned, the Zuiderzee has been used only as an exceedance tool (i.e., as a  
455 maximum setup threshold for coastal construction), while here it is applied in a predictive  
456 capacity and thus is not a traditional application of the parameterization.

457

458 The hysteresis associated with maximum wind speed and peak setup was investigated for all  
459 three wind forcing methods (Section 2.4). Cross correlation revealed that the peak setup lagged  
460 the maximum wind speed by 6 hours for both the top of the hour and the hourly mean methods  
461 while indicating little or no lag for the wind run method. This latter result is consistent with the  
462 averaging methodology of this approach which is based on a non-centered running mean that  
463 shifts the wind forcing forward in time and thus has an intrinsic lag.

464

465 While all of the parameterizations generally perform quite well in predicting the setup between  
466 the two locations, a hydrodynamic model simulation is necessary in order to provide context  
467 with respect to the lagoon-wide impact. The coupled ADCIRC + SWAN simulation indicates  
468 that the water level response is relatively uniform between Titusville and Sebastian Inlet (Fig. 1),  
469 and produced comparable results, in terms of timing, to those of the parameterizations. However,  
470 the model also underpredicted the peak setup for the event, which was attributed to the WRF  
471 generated wind forcing (Weaver et al., 2016b).

472

473 An examination of some of the poorly predicted setup events indicates that these cases may, in  
474 part, be related to relatively large air-water temperature differences. While the near surface  
475 atmospheric stability will impact the surface stress, it has not been considered here. A follow-up



476 study regarding the role of stability in the generation of estuary setup would likely improve the  
477 forecasts.

478  
479 The goal of this study was the development of a setup parameterization, along with an  
480 appropriate wind forcing, in support of real time water level forecasting on a coastal estuary.

481 This work is part of a larger effort to integrate NCEP ensemble model output (winds) within the  
482 NWPS. After accounting for bias correction, downscaled wind forecasts from the SREF or GEFS  
483 can be used to force a setup parameterization. In addition to providing an inexpensive water level  
484 ensemble, the results would serve as a guide for the NWS in terms of allocating resources for a  
485 high resolution (deterministic) hydrodynamic model simulation for high impact events.

486 **Acknowledgements**

487 Funding: The work in this paper was supported with funds from NOAA and the National  
488 Weather Service Program Office (NWSPO), Collaborative Science, Technology, and Applied  
489 Research (CSTAR) Award: NA14NWS4680014, “*An Ensemble-based Approach to Forecasting*  
490 *Surf, Set-Up and Surge in the Coastal Zone*”.

491

492 Water level data from pressure gauges installed in the IRL by the Florida Institute of Technology  
493 were supplemented with data from gauges managed by the Saint John’s River Water  
494 Management District (SJRWMD).

495 **References**

496

497 Ahrens, J.P., 1976. Overlay of Large, Placed Quarrystone and Boulders to Increase Riprap

498 Stability. Fort Belvoir, VA.

499 Apotsos, A., Raubenheimer, B., Elgar, S., Guza, R.T., 2008. Testing and calibrating parametric

500 wave transformation models on natural beaches. *Coast. Eng.* 55, 224–235.

501 <https://doi.org/10.1016/j.coastaleng.2007.10.002>

502 Booij, N., Rc, Lh, 1999. A third-generation wave model for coastal regions-1. Model description

503 and validation. *J. Geophys. Res. - Ocean.* 104 (C4), 7649–7666.

504 Csanady, G., 1973. Wind induced barotropic Motions in long lakes. *J. Phys. Oceanogr.*

505 [https://doi.org/10.1175/1520-0485\(1973\)003<0429:WIBMIL>2.0.CO;2](https://doi.org/10.1175/1520-0485(1973)003<0429:WIBMIL>2.0.CO;2)

506 Dean, R.G., Dalrymple, R.A., 1991. *Water Wave Mechanics for Engineers and Scientists*. World

507 Scientific Publishing Co Inc.

508 Du, J., Tracton, M.S., 2001. Implementation of a real-time short range ensemble forecasting

509 system at NCEP: An update. pp. 355–360.

510 Freeman, J.C., Baer, L., Jung, G.H., 1957. The bathystrophic storm tide. Sears Foundation for

511 Marine Research.

512 Harris, D.L., 1963. Characteristics of the hurricane storm surge, Weather Bureau Technical

513 Papers. Department of Commerce, Weather Bureau.

514 Holman, B.P., Lazarus, S.M., Splitt, M.E., 2017. A fetch-based statistical method to bias correct

515 and downscale wind speed over unresolved water bodies. *Weather Forecast.* WAF-D-17-

516 0016.1. <https://doi.org/10.1175/WAF-D-17-0016.1>

517 Kjerfve, B., 1986. Comparative oceanography of coastal lagoons. *Estuar. Var.* 63–81.

518 <https://doi.org/10.1016/B978-0-12-761890-6.50009-5>

519 Luettich, R.A., Jr., J.J. Westerink, and N.W.S., 1992. ADCIRC: an advanced three-dimensional  
520 circulation model for shelves coasts and estuaries, report 1: theory and methodology of  
521 ADCIRC-2DDI and ADCIRC-3DL, Dredging Research Program Technical Report DRP-  
522 92-6, U.S. Army Engineers Waterways Experiment Station, Vicksburg, MS,.

523 Mostertman, L.J., 1963. Waves of long and short period. Van Douwen, AA Sel. Asp. Hydraul.  
524 Eng. Lib. Amicorum Dedic. to Johannes Theodoor Thijsse, Occas. his Retire. as Profr.

525 Reynolds-Fleming, J. V., Luettich, R.A., 2004. Wind-driven lateral variability in a partially  
526 mixed estuary. *Estuar. Coast. Shelf Sci.* 60, 395–407.  
527 <https://doi.org/10.1016/j.ecss.2004.02.003>

528 Saville Jr, T., 1952. Wind Set-Up and Waves in Shallow Water.

529 Smith, N.P., 1990. Computer simulation of tide-induced residual transport in a coastal lagoon. *J.*  
530 *Geophys. Res.* 95, 18205–18211. <https://doi.org/10.1029/JC095iC10p18205>

531 Sorensen, R.M., 2006. Basic Coastal Engineering Basic Coastal, Environmental Engineering.  
532 Springer Science & Business Media. <https://doi.org/10.1007/b101261>

533 Toth, Z., Kalnay, E., 1993. Ensemble forecasting at NMC: The generation of perturbations. *Bull.*  
534 *Am. Meteorol. Soc.* 74, 2317–2330. [https://doi.org/10.1175/1520-](https://doi.org/10.1175/1520-0477(1993)074<2317:EFANTG>2.0.CO;2)  
535 [0477\(1993\)074<2317:EFANTG>2.0.CO;2](https://doi.org/10.1175/1520-0477(1993)074<2317:EFANTG>2.0.CO;2)

536 van der Westhuysen, A.J., Padilla, R., Santos, P., Gibbs, A., Gaer, D., Nicolini, T., Tjaden, S.,  
537 Devaliere, E.-M., Tolman, H., 2013. Development and validation of the Nearshore Wave  
538 Prediction System. *Proc. 93rd AMS Annu. Meet.* 2013.  
539 [https://doi.org/10.3319/TAO.2009.04.16.01\(IWNOP\).Tolman](https://doi.org/10.3319/TAO.2009.04.16.01(IWNOP).Tolman)

540 van Dorn, W.G., 1953. Wind stress on an artificial pond. *J. Mar. Res.* 12, 249–276.

541 Weaver, R.J., Johnson, J.E., Ridler, M., 2016a. Wind-Driven Circulation in a Shallow Microtidal

542 Estuary: The Indian River Lagoon. *J. Coast. Res.* 322, 1333–1343.  
543 <https://doi.org/10.2112/JCOASTRES-D-15-00046.1>

544 Weaver, R.J., Taeb, P., Lazarus, S., Splitt, M., Holman, B.P., Colvin, J., 2016b. Sensitivity of  
545 modeled estuarine circulation to spatial and temporal resolution of input meteorological  
546 forcing of a cold frontal passage. *Estuar. Coast. Shelf Sci.* 183, 28–40.  
547 <https://doi.org/10.1016/j.ecss.2016.10.014>

548 Wu, J., 1969. Wind stress and surface roughness at air-sea interface. *J. Geophys. Res.* 74, 444–  
549 455. <https://doi.org/10.1029/JB074i002p00444>

550